DR. FRANCIS E. WASHER
National Bureau of Standards
Washington, D.C. 20234

Resolving Power Related to Aberration

The resolving power of a lens can be predicted on the basis of chromatic and spherical aberration.

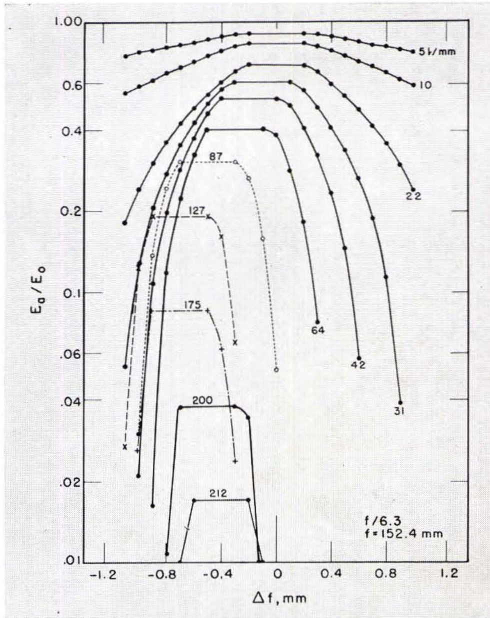

FRONTISPIECE, E_a/E_o *vs.* Δf at selected values of resolving power A. These curves indicate the manner in which contrast at a given value of A in the image varies with displacement from the plane of best paraxial focus F_o for a lens having both longitudinal chromatic aberration d_c and longitudinal spherical aberration $\Delta f'$. (See text page 225.)

(Abstract on next page)

1.0 INTRODUCTION

WHEN THE MEASURED VALUES of resolving power of a lens are compared with the theoretical values predicted by diffraction theory, the measured values are usually appreciably lower than the theoretical. In addition, the measured depth of focus in the image space is usually greater than would be expected on the basis of simple theory. This paper presents an heuristic approach to this problem that leads to a plausible explanation of the apparent deviation of measured from theoretical values of resolving power.

It has been found that when due allowance is made for factors that may influence contrast in the image such as area of lens contributing to resolution, longitudinal chromatic, and longitudinal spherical aberration there is then good agreement between theoretical and measured values of the resolving power. It is also found that this approach leads to a clear understanding of such phenomena as sharp decline in the contrast between light and dark lines of a line pattern with decreasing line separation; change in position of best focus with changing line separation; and anomalous variations in contrast with decreasing line separation for differing position of the focal plane.

2.0 THEORY FOR IDEAL LENS

Before proceeding to a discussion of the effects of relative lens area and aberrations on resolving power, it is necessary to review briefly relations connecting resolving power and depth of focus with f-number of the lens and the wavelength of the image-forming light for an ideal lens. These relations are described in detail in earlier publications[1,2] and the present brief review is included to permit better understanding of the problem.

2.1 RESOLVING POWER FOR AN IDEAL LENS

In the case of photographic lenses, resolving power is usually determined by examination of an image formed by the lens of a series of patterns of dark and light lines of equal widths and known separations. The line separation varies from pattern-to-pattern by a known ratio. In the image, each pattern is characterized by a value of A expressed in lines/mm which is given by the relation

$$A = \frac{1}{d} \text{ lines/mm} \tag{1}$$

where d is the measured line separation in the image. When the image is examined, the observer will note that the lines in the coarsest patterns (small A) are clearly resolved while those in the finest patterns (large A) are definitely not resolved. For some intermediate pattern (A_o), the observer will note that the lines in the pattern A_o are just barely resolved while the lines are not resolved in any of the patterns where A is greater than A_o and the lines are clearly resolved in all of the patterns where A is less than A_o. The value A_o is accepted as the maximum value of the resolving power of the lens.

ABSTRACT: *An heuristic method accounts for the discrepancy between measured and theoretical values of resolving power of lenses. The analysis also accounts for the sharp decline in contrast with increasing values of resolving power expressed in lines per mm in the image plane. Resolutions and contrast are affected by the fraction of the lens area transmitting image-forming light, longitudinal chromatic aberration, and longitudinal spherical aberration. An example demonstrates change in focus with change in resolving power and shows how it is readily explained on the basis of simple diffraction theory.*

For an ideal lens the maximum value A_o of the resolving power* may be determined from theoretical considerations and is as follows:

$$A_o = \frac{1}{1.22b\lambda} \text{ lines/mm} \qquad (2)$$

where b is the f-number of the lens and λ is the wavelength of the incident light. For a wavelength of $\lambda = 585.4$ mμ, the value of A_o is

$$A_o = \frac{1400}{b} \text{ lines/mm.} \qquad (3)$$

The relations given in Equations 2 and 3 are valid only for imagery in the axial region. In the extra-axial region, two additional relations are necessary. These relations, for the maximum resolving power for tangential lines, A_{t_β}, and for the maximum resolving power for radial lines, A_{r_β}, are given by the expressions

$$A_{t_\beta} = A_o \cos^3 \beta \qquad (4)$$

and

$$A_{r_\beta} = A_o \cos \beta$$

where β is the angular separation of the image from the axis and A_o is the maximum axial resolving power given by Equation 2.

* NOTE: In this presentation, the term resolving power A simply indicates the number of lines/mm in a given line pattern in the image. It refers to a resolved pattern when $A < A_o$ and to an unresolved pattern when $A > A_o$. The value of resolving power associated with the limit of resolution of the lens is always designated A_o.

2.2 LIMITATIONS ON USE OF THEORETICAL VALUES OF RESOLVING POWER

The values of the resolving powers shown in the preceding section are theoretical values and are valid only for an ideal lens used under ideal conditions. These values are sometimes criticized as being unrealistic because much lower values are commonly found for actual lenses. This criticism sometimes proceeds to the point of suggesting the total elimination of the concept of resolving power as a criterion for use in judging the image-forming properties of lenses. This criticism is based for the most part on a misunderstanding of the term and an overlooking of the conditions under which these theoretical values are valid.

Much discussion of the effect of contrast and its effect on imagery usually occurs in the criticism of resolving power. A little thought on the manner of derivation of the theoretical values of resolving power would bring out the fact that the concept of contrast is implicit in the original derivation which is valid for two bright point sources of light simulating close stars against a dark background. Hence, the relations are restricted to conditions of high or infinite contrast between the point sources and their background. It is self evident that the ability to distinguish between close points will diminish with decreasing contrast between the points and the background and the resolving power will be zero when there is no contrast between the points and the background.

It is nonetheless desirable to know the ultimate value of resolving power attainable under ideal conditions if for no other reason than to avoid the pitfall of trying to achieve a higher order of definition than is theoretically possible for the conditions specified. An example of this is setting a requirement that a given lens to be acceptable must resolve detail of the order of 200 lines/mm when operating at a relative aperture of $f/11$ at which aperture the theoretical maximum is 127 lines/mm.

In point of fact many lenses will achieve the theoretical maximum values of resolving power at relative apertures ranging from $f/8$ to $f/64$ when measurements are made visually using high contrast targets. At larger stop openings, the quality of imagery is degraded by the presence of aberrations such as longitudinal spherical and chromatic. In the extra-axial region, curvature of field and astigmatism tend to reduce the values of resolving power observed in the plane of best axial focus.

In addition to lens aberrations, the nature of the receptor reduces the magnitude of observed values of resolving power. Different photographic emulsions will yield different values of resolving power under identical conditions. Variation of the contrast further changes the values of observed resolving power.

It is clear therefore that the ability of a lens to resolve close objects is a function of not one but of many factors. These factors include target contrast, relative aperture of lens, orientation of lines in linear pattern in the extra-axial region, angle of separation from axis, curvature of field, selection of focal plane, lens aberration, and nature of the receptor. It is usually not possible to control all of these factors within desirable limits. However, if the measured value of the resolving power at high target contrast is known for a given lens, it is possible to determine its probable performance under a wide variety of operating conditions. This is particularly true if one also has available measured values of curvature of field and longitudinal spherical aberration.

2.3 DEPTH OF FOCUS FOR AN IDEAL LENS

When a lens forms an image of an object in front of the lens, there is a small finite range on the axis in the image space in which a recognizable image of the object is formed. The focal point of the lens lies within this range usually near the center. This range is called "depth of focus" and refers to the distance measured along the axis in the image space that may be traversed without the resolving power A measured in the image plane falling below an arbitrarily selected value in the range 0 to A_o. Depth of focus is not to be confused with "depth of field" which refers to the range in the object space for which all point objects are imaged with a radius of the circle of confusion remaining less than or equal to some arbitrarily selected value.

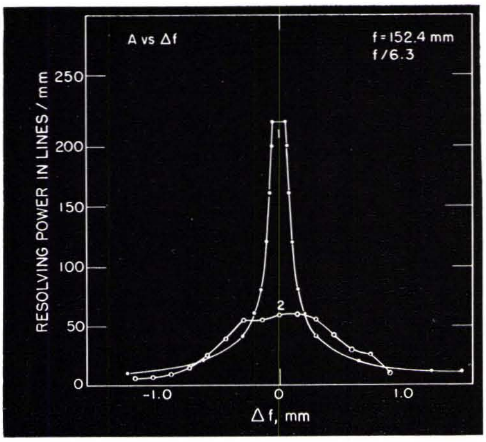

FIG. 1. Axial resolving power *vs.* displacement Δf of the image plane from the plane of best axial focus for an $f/6.3$ lens having a focal length of 152.4 mm. Curve 1 shows the variation in resolving power for an ideal lens for $\lambda = 585.4$ mμ. The curve marked 2 shows the measured values obtained photographically using V-F emulsion and long-line high contrast resolution test charts.

It can be shown that the depth of focus d_f in millimeters can be computed from the relation

$$d_f = \frac{4b}{A} \tag{5}$$

where b is the f-number and A is the resolving power in lines/mm for which the depth of focus is to be determined. Equation 5 is based on geometric optics and is restricted to values of A lying between 0 and A_o where A_o is computed from Equation 2. The value of d_f is independent of angular separation from the axis for a given f-number. Hence no additional equations for the off-axis conditions are necessary.

3.0 MEASURED AND THEORETICAL VALUES OF RESOLVING POWER

It is of interest to compare the measured and theoretical values of resolving power in a succession of focal planes extending through the region of usable imagery of a lens having a focal length of 152.4 mm and relative aperture of $f/6.3$. The theoretical values of resolving power for a series of focal planes separated by distance Δf from the plane of best focus were computed with the aid of Equations 3 and 5. The computed variation of theoretical resolving power with Δf is shown as Curve 1 in Figure 1. The measured values were obtained photographically using Eastman Spectroscoper Plates, Emulsion V-F. The light incident on the lens was produced by a tungsten source with a Wratten K-3 filter used between the source and the high contrast long-line resolution chart. The variation in measured resolving power with Δf is shown as Curve 2 in Figure 1.

It is clear from the graph that the theoretical maximum resolving power A_o is markedly higher than the measured value of A_o. In addition, the theoretical values of A are higher than the measured values over an appreciable range of values of Δf in the vicinity of $\Delta f=0$. The substantially lower values for Curve 2 cannot be attributed solely to limitations of the emulsion as the limiting resolving power of the emulsion is at least two times greater than the maximum observed value of A. It is also noteworthy that the depth of focus for some of the lower values of A is greater than the depth of focus indicated for the predicted values of A.

4.0 Correlation of Observed and Theoretical Values of the Resolving Power

The pronounced difference in magnitude frequently found between observed and theoretical values of the resolving power has tended to cause some investigators to discount the usefulness of resolving power measurements. A great deal of recent work is devoted to the evaluation of such quantities as the *contrast transfer function* which describes the variation in contrast between the light and dark lines of a resolution test chart as the separation of lines varies from some selected finite value to zero. In the evaluation of this quantity the variation of contrast in the initial target pattern must be known and that in the final image must be determined for each value of line separation. From these two quantities the reduction in contrast with decreasing line separation may be determined for a given set of conditions. In the interpretation of the final results, recourse is had to harmonic analysis with the result that an extensive mathematical structure has been built up around the phenomenon of reduction in target contrast with decreasing line separation.

The foregoing type of analysis has proved useful in many problems concerning lens performance and is eminently satisfactory to those skilled in the use thereof. However, it is frequently unclear in its relating of known optical quantities such as lens aberration to observed characteristics of the image.

In the present section, an attempt is made to show that many of the observed characteristics of the image can be explained by diffraction theory alone together with reasonably plausible hypotheses concerning the effect of aperture, depth of focus, longitudinal chromatic, and longitudinal spherical aberration. The reasoning is based on the assumption that the contrast between lines in the target object is extremely high.

4.1 Effect of Aperture on Resolution

When images of a series of patterns characterized by values of the resolving power A ranging from 0 to A_o are formed by a lens, it is of interest to determine the fractional portion of the lens aperture that contributes to image formation for any one of the patterns. For a circular aperture, the quantity of light flux E transmitted by the lens is determined by the aperture area $K=\pi h^2$ where h is the radius of the aperture and the limit of resolution A_o is determined by the aperture diameter, $D=2h$. The expression for maximum resolving power given in Equation 3 may be written

$$A = \frac{2800h}{f} \qquad (6)$$

where $2h/f$ is substituted for $1/b$.

When a uniformly illuminated test chart having constant contrast between light and dark lines of all patterns is imaged by a lens all patterns in the image are resolved up to the limit set by Equation 6. If the maximum aperture is h_o, all values of A from 0 to A_o are present in the image. For an intermediate aperture of radius $h_1 < h_o$, values of A ranging from 0 to A_1 are obtained where A_1 is less than A_o. However, patterns requiring resolving powers lying between A_1 and A_o are not resolved at this reduced aperture of radius h_1. If now the aperture is increased to h_o and a circular opaque disk of radius h_1 is so placed in front of the lens that the transmitting area of the aperture is the annular zone of inner radius h_1 and outer radius h_o, then all values of A lying between 0 and A_o are again present in the image. It is therefore reasonable to assume that, when the lens is operating at full aperture, the light energy E that contributes to the formation of images having resolving powers between A_1 and A_o is drawn from the annular region of inner radius h_1 and outer radius h_o. It is also reasonable to assume that light transmitted by the circular area of radius h_1 does not contribute to the formation of images having resolving powers in the range from A_1 to A_o. However, it is probable that the light transmitted by the area of radius h_1 may contribute to the blur light and so reduce the contrast in the images of those patterns having resolving powers between A_1 and A_o.

To determine the ratio of the energy content E_a of the light flux contributing to the formation of the image of pattern A to the energy content E_o of all light transmitted by the aperture of radius h_o coming from the target pattern A, it is assumed that E_a is proportional to the annular area $K_a = \pi(h_o^2 - h_1^2)$ and E_o is proportional to the total area $K_o = \pi h_o^2$ where

$$\frac{E_a}{E_o} = \frac{K_a}{K_o} = \frac{h_o^2 - h_1^2}{h_o^2}. \qquad (7)$$

It is convenient to express K_a/K_o in terms of the resolving powers A_1 and A_o. This may be done with the aid of Equation 6 which leads to the expression

$$\frac{E_a}{E_o} = \frac{K_a}{K_o} = \frac{A_o^2 - A_1^2}{A_o^2}. \qquad (8)$$

For example, an $f/2$ lens resolves 700 lines/mm at full aperture, 500 lines/mm with the aperture reduced to $f/2.8$, and 350 lines/mm with the aperture reduced to $f/4$. Using Equation 8, one would infer that with the lens set at maximum aperture the values of E_a/E_o at $A = 700$, 500 and 350 lines/mm would be 0.00, 0.49 and 0.75 respectively. The contrast in the image would therefore be a maximum at $A = 0$ and decrease steadily with increasing A until it reaches zero at $A = A_o$.

To illustrate this effect of aperture upon the manner in which E_a/E_o varies with resolving power A, values of K_a/K_o have been calculated with the aid of Equation 8 for a series of values of A for an $f/6.3$ lens having a focal length of 152.4 mm. These values of K_a/K_o are listed in Table 1. From the table, it is evident that only 19% of the total lens area contributes image-forming light in the formation of the image of the 200 line/mm pattern while nearly 100% of the total lens area contributes to image formation for the 10 line pattern. It is clear from the foregoing analysis that the decrease in the ratio of aperture area available for supplying image-forming light to total aperture area may well account for a major portion of the reduction in image contrast with increasing values of A.

It is also clear that the areal effect alone is not sufficient to reduce the theoretically possible values of resolving power for the plane of best focus down to the magnitude of the observed values.

4.2 EFFECT OF DISPLACEMENT OF THE FOCAL PLANE

It has been shown that for the plane of best focus, the ratio of the energy E_a of the light available for imaging a pattern of resolving power A to the total energy E_o associated with that value of A and transmitted by the lens is given by Equation 8 when effect of available area alone is considered. However if the imagery in a plane f_o separated by amount Δf from the plane of best focus F_o is examined, markedly lower values of A are found. Moreover, the manner in which image contrast changes with increasing A also changes with increasing Δf indicating that a factor related to depth of focus is also operative in lowering the contrast.

Consider the graphical presentation of depth of focus as a function of resolving power A for an ideal lens of aperture $f/6.3$ which is shown in Figure 2. The mid plane of the region of usable imagery is indicated by the ordinate passing through the abscissa F_0 which therefore marks the plane of best definition. The limits of the region of usable imagery are bounded by the curves F_1 and F_2 where

$$F_1 = F_o - \frac{d_f}{2} = F_o - \frac{2b}{A} \qquad (9)$$

and

$$F_2 = F_o + \frac{d_f}{2} = F_o + \frac{2b}{A} \qquad (10)$$

where b is the maximum f-number and A is a value of the resolving power in the range 0–A_o. It is obvious that

$$F_2 - F_1 = d_f = \frac{4b}{A} \qquad (11)$$

where d_f is the depth of focus at any value of A. The values of $(F_1 - F_o)$ and $(F_2 - F_o)$ used in plotting Figure 2 were calculated using Equations 9 and 10 and are listed in Table 1. This table also lists the values of the depth of focus d_f obtained with the aid of Equation 11.

Consider now an image plane f_o displaced by distance Δf from F_o and whose position with respect to F_o is indicated in Figure 2A by the line passing through abscissa f_o. Limiting curves f_1 and f_2 can be drawn with respect to f_o where

$$f_1 = f_o - \frac{2b}{A} \qquad (12)$$

and

$$f_2 = f_o + \frac{2b}{A}. \qquad (13)$$

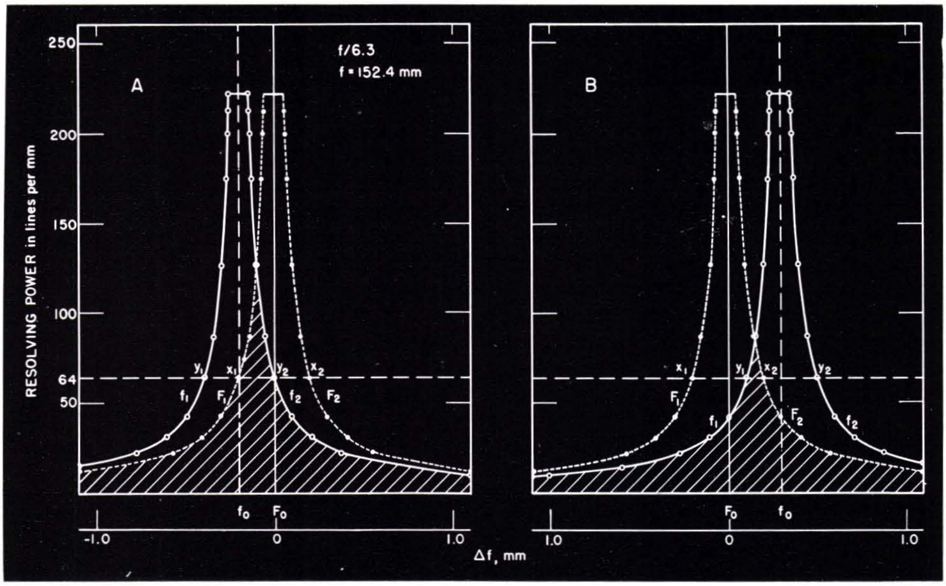

FIG. 2. Axial resolving power *vs.* Δf for an ideal lens. Curves F_1 and F_2 mark the bounds of the region of usable imagery with respect to the plane of best definition F_o. For an image plane f_o distant Δf from F_o, the curves f_1 and f_2 show the limiting depth of focus for each value of A. In Box A, the shaded area shows the region of usable imagery common to both f_o and F_o for $\Delta f=(f_o-F_o)=-0.2$ mm. In Box B, similar information is given for $\Delta f=0.3$ mm.

It is hypothesized that, if any image-forming light associated with a given value of A lies within the bounds set by the curves f_1 and f_2, then imagery for that value of A will occur in the plane f_o. It is accepted that image-forming light conforming to this requirement does exist in the region of usable imagery bounded by the curves F_1 and F_2. It is therefore reasonable to suppose that the region common to both the region bounded by f_1 and f_2 and to that bounded by F_1 and F_2 represents that portion of the image-forming light capable of being imaged in f_o. The region common to both is shown as the shaded area under the curves for two values of $\Delta f=f_o-F_o$ in Figure 2. It is clear from the figure that the quantity of light available for image formation in the plane f_o is less than that available in plane F_o. It is assumed that the ratio of reduction of image-forming light at a given value of A from F_o to f_o is the same as the ratio of the common depth of focus to the total depth of focus for F_o. This may be visualized with the aid of Figure 2A where a line drawn parallel to the axis of abscissae at an ordinate height A cuts curves F_1 and F_2 at x_1 and x_2 and intersects curves f_1 and f_2 at y_1 and y_2. The line x_1y_2 is the focal depth common to both, and the line x_1x_2 is the depth of focus for the plane of best focus F_o. The ratio of reduction is j_a/j_o where $j_a=x_1y_2$ in Figure 2A and y_1x_2 in Figure 2B and $j_o=x_1x_2$ in both cases. Hence for negative values of Δf

$$\frac{j_a}{j_o}=\frac{x_1y_2}{x_1x_2} \tag{14}$$

TABLE 1

Range of the region of usable imagery with respect to the plane of best focus F_o for an ideal lens as a function of resolving power A for an $f/6.3$ lens. Values of the depth of focus $d_f=j_o$ and the ratio K_a/K_o are also listed.

A	F_1-F_o	F_2-F_o	F_2-F_1	$\frac{A_o^2-A^2}{A_o^2}$
	$-d_f/2$	$+d_f/2$	$d_f=j_o$	K_a/K_o
lines/mm	mm	mm	mm	
5	−2.520	2.520	5.040	1.000
10	−1.260	1.260	2.520	.998
22	−0.575	0.575	1.150	.990
31	− .406	.406	0.812	.980
42	− .297	.297	.594	.964
64	− .198	.198	.396	.918
87	− .144	.144	.288	.845
127	− .099	.099	.198	.672
175	− .072	.072	.144	.381
200	− .063	.063	.126	.188
212	− .059	.059	.118	.088
222	− .057	.057	.114	.000

and for positive values of Δf

$$\frac{j_a}{j_o} = \frac{y_1 x_2}{x_1 x_2} \cdot \quad (15)$$

From the graph and Equations 9 and 10, it is clear that

$$j_o = x_1 x_2 = F_2 - F_1 = \frac{4b}{A} \cdot \quad (16)$$

For negative values of $\Delta f = f_o - F_o$

$$j_a = x_1 y_2 = f_2 - F_1 = \Delta f + \frac{4b}{A} \quad (17)$$

and for positive values of Δf

$$j_a = y_1 x_2 = F_2 - f_1 = \frac{4b}{A} - \Delta f. \quad (18)$$

For negative values of Δf, the ratio j_a/j_o is

$$j_a/j_o = 1 + \frac{A\Delta f}{4b} \quad (19)$$

and for positive values of Δf

$$j_a/j_o = 1 - \frac{A\Delta f}{4b} \cdot \quad (20)$$

Values of $(f_1 - F_o)$ and $(f_2 - F_o)$ as a function of A for an $f/6.3$ lens for the case

$$\Delta f = (f_o - F_o) = -0.2 \text{ mm}$$

are listed in Table 2 and are plotted as curve $f_1 f_2$ in Figure 2A. These values were calculated with the aid of Equations 12 and 13. Values of j_a and j_a/j_o computed with the aid of Equations 17 and 18 are also listed in Table 2. Similar values of $(f_1 - F_o)$ and $(f_2 - F_o)$ for the case $\Delta f = 0.3$ mm are shown in Figure 2B.

While contrast in the image for a given value of A is reduced in amount j_a/j_o because of the displacement Δf from F_o, it must be remembered that area effect discussed in Section 4.1 is also operative. The combined effect is obtained by multiplying the quantitites j_a/j_o and K_a/K_o, so the equation for E_a/E_o becomes

$$\frac{E_a}{E_o} = \frac{j_a}{j_o} \cdot \frac{K_a}{K_o} \cdot \quad (21)$$

The evaluation of E_a/E_o for values of $\Delta f = -0.2$ mm is shown in Table 2. For $\Delta f = 0$, the values of E_a/E_o are the same as the values of K_a/K_o listed in Table 1. The manner in which E_a/E_o varies with A for these three values of Δf is shown in Figure 3. The variation of E_a/E_o with Δf at selected values of A for the entire region of usable imagery can be readily computed in the foregoing manner. This has been done for an ideal lens of relative aperture $f/6.3$ and the results are presented in Figure 4.

4.3 EFFECT OF LONGITUDINAL CHROMATIC ABERRATION

Longitudinal chromatic aberration produces a displacement of the plane of best focus with change in the wavelength of the incident light. For lenses of the type described in Table 2, the over-all displacement d_c may range from 0.5 to 0.7 mm for the spectral region normally used. It seems probable that the presence of longitudinal chromatic aberration may contribute to lowered resolving power and changes in the depth of focus. In Figure 5, the region of usable imagery for a given central wavelenth λ_c is shown bounded by the curves F_1 and F_2 computed with the

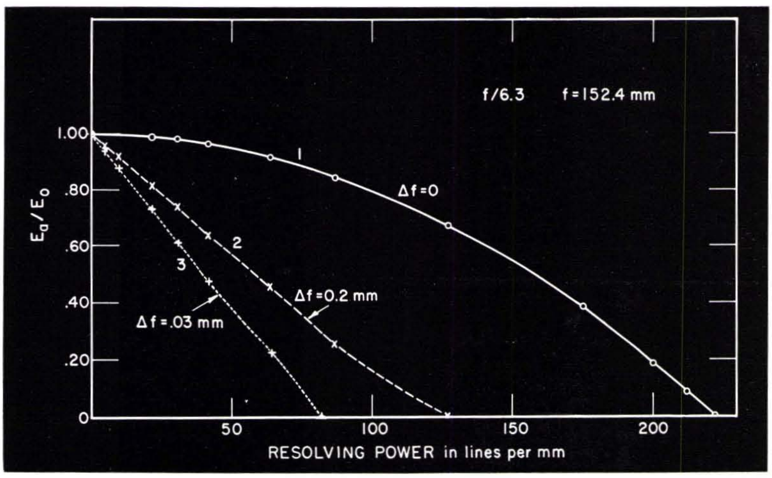

FIG. 3. E_a/E_o *vs.* resolving power A for an image plane f_o separated by distance Δf from plane of optimum focus F_o. Results are shown for three values of Δf: (1) 0.00, (2) ± 0.20, and (3) ± 0.30 mm.

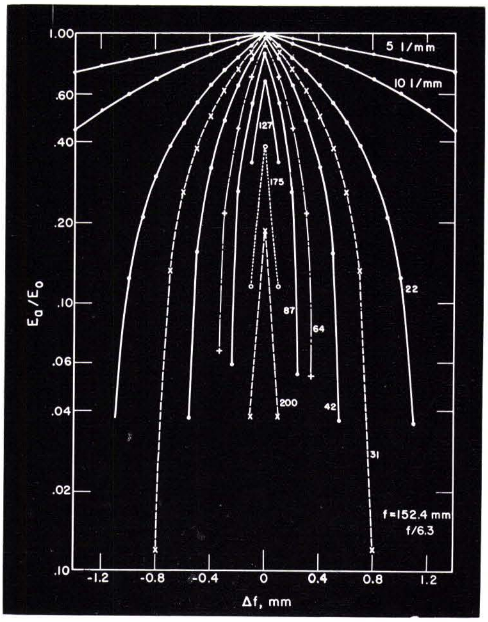

FIG. 4. E_a/E_o *vs.* Δf at selected values of resolving power A. These curves indicate the manner in which contrast in the image varies with displacement of the image plane f_o from the plane of best focus F_o for an ideal lens.

aid of Equations 9 and 10 with the zero of abscissae shifted so that $F_o=0$. One may assume that at some wavelength λ_b at the lower wavelength limit of the used spectral region the displacement of the focal plane may be toward the lens to F_o' by amount $-d_c/2$. Curves may be drawn F_1' and F_2' that bound the region of usable imagery for the focal plane located at $(F_o'-F_o)=-d_c/2$.

TABLE 2

Range of focus as a function of resolving power A for the image plane f_o referred to the plane of best focus F_o where $\Delta f=(F_o-f_o)=-0.2$ mm. Values of the focal range common to both f_o and F_o are listed as j_a. Values of the ratios j_a/j_o and E_a/E_o are also listed. The values are for an $f/6.3$ lens.

A	f_1-F_0	f_2-F_0	j_a	j_a/j_0	E_a/E_0
lines/mm	mm	mm	mm		
5	−2.720	2.320	4.840	0.960	0.960
10	−1.460	1.060	2.320	.921	.919
22	−0.775	0.375	0.950	.826	.818
31	−.606	.206	.612	.754	.739
42	−.497	.097	.394	.663	.639
64	−.398	−.002	.196	.495	.454
87	− 344	−.056	.088	.306	.259
127	−.299	−.101	−.002	.000	.000
175	−.272	−.128			
200	−.263	−.137			
212	−.259	−.141			
222	−.257	−.143			

$j_a=(f_2-F_1)=(f_2-F_0)-(F_1-F_0)$

In a similar manner, one may assume that at some other wavelength λ_r at the upper wavelength limit of the used spectral region the displacement may be away from the lens by amount $d_c/2$ to F_o''. Curves F_1'' and F_2'' may be drawn that bound the region of usable imagery for the focal plane located at $(F_o''-F_o)=+d_c/2$. This process can be continued for all intermediate wavelengths and the entire region filled with boundary curves. The outermost envelope that encompasses the entire region will be the curves F_1' and F_2'' defined by the equations

$$F_1' = F_o - \tfrac{1}{2}(d_f + d_c) \tag{22}$$

and

$$F_2'' = F_o + \tfrac{1}{2}(d_f + d_c). \tag{23}$$

These curves are identical in form to those given in Equations 9 and 10 except for the addition of the constant d_c which is the overall displacement of the focus arising from longitudinal chromatic aberration.

Assuming uniform intensity throughout the used range of λ, it is reasonable to suppose that the same method of analysis used in Section 4.2 in evaluating the ratio j_a/j_o for

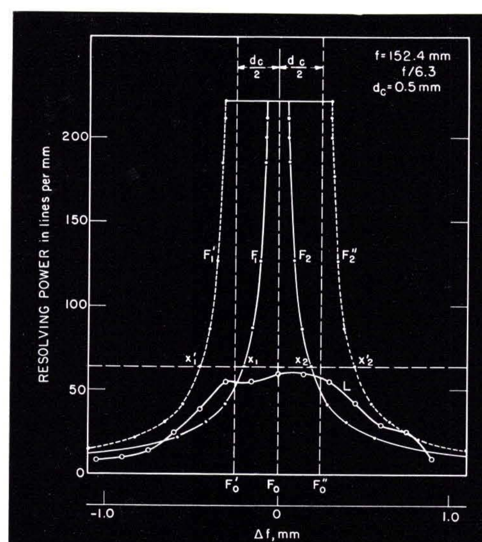

FIG. 5. Axial resolving power *vs.* Δf for a lens affected by longitudinal chromatic aberration d_c. Curves F_1 and F_2 mark the bounds of the region of usable imagery for the plane of best definition F_o for light of central wavelength $\lambda=\lambda_c$. Curve F_1' marks the lower limit of usable imagery for the plane of best definition F_o' for $\lambda=\lambda_b=\lambda_c-\Delta\lambda$ and curve F_2'' shows the upper limit of usable imagery for the plane of best definition F_o'' for $\lambda=\lambda_r=\lambda_c+\Delta\lambda$. $(F_o-F_o')=d_c/2=(F_o''-F_o)$. The curve marked L shows values of A *vs.* Δf for an actual lens determined by photographic methods.

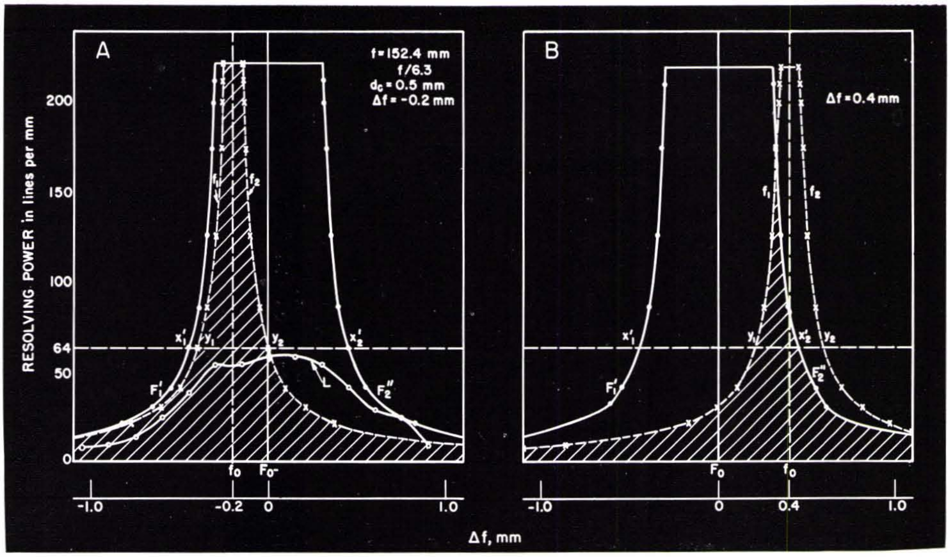

FIG. 6. Axial resolving power A vs. Δf for a lens affected by longitudinal chromatic aberration d_c. Curves F_1' and F_2'' mark the bounds of the region of usable imagery. F_o locates a focal plane lying in the center of the range of best focus. For an image plane f_o distant Δf from F_o, the curves f_1 and f_2 show the limiting depth of focus with respect to f_o for each value of A. In Box A, the shaded area shows the region of usable imagery common to f_o and the region enclosed by F_1' and F_2'' for $\Delta f=(f_o-F_o)=-0.2$ mm. Similar information for $\Delta f=0.4$ mm. is shown in Box B.

an image plane displaced by amount Δf from F_o can be used in evaluating this ratio modified to incorporate the displacement d_c.

To aid in the analysis, values of F_1' and F_2'' have been calculated with the aid of Equations 22 and 23 for an $f/6.3$ lens having longitudinal chromatic aberration in amount $d_c=0.50$ mm. These values are listed in Table 3 and are shown graphically in Figure 6. The limiting bounds f_1 and f_2 of the region of usable imagery for an image plane f_o separated by distance $\Delta f=(f_o-F_o)=-0.2$ mm are also drawn in Figure 6A. The values of f_1 and f_2 are taken from Table 2. For this case where $\Delta f<d_c/2$, the shaded area in the graph representing the region of imagery common to both F_o and f_o is completely enclosed by the limits F_1' and F_2''. Using the method of analysis given in Section 4.2, the ratio j_a/j_o is

$$\frac{j_a}{j_o}=\frac{y_1y_2}{x_1'x_2'}=\frac{d_f}{d_f+d_c}\cdot \tag{24}$$

Inserting the value of j_a/j_o from Equation 24 into Equation 21, the value of E_a/E_o becomes

$$\frac{E_a}{E_o}=\frac{d_f}{d_f+d_c}\cdot\frac{K_a}{K_o}\cdot \tag{25}$$

This clearly shows that for a given value of A the value of E_a/E_o decreases with increasing d_c. Values of E_a/E_o for $d_c=0.50$ are listed in Table 3, and shown graphically in Figure 7. Values of E_a/E_o for $d_c=0$ are also shown in the Figure 7. Comparison of the two curves shows clearly that longitudinal chromatic aberration produces marked reduction in the values of E_a/E_o. It is also worthy of note that at a given value of A value E_a/E_o is constant for a constant value of d_c over a vocal range Δf where

$$\frac{-d_c}{2}\leq\Delta f\leq\frac{d_c}{2}\cdot \tag{26}$$

TABLE 3

Range of the region of usable imagery with respect to the plane of best focus F_o (for $\lambda=\lambda_c$) as a function of resolving power A for an $f/6.3$ lens with longitudinal chromatic aberration $d_c=0.50$ mm. Values of $j_o=d_f+d_c$, the quantity j_a/j_o for $j_a=d_f$, and the values of E_a/E_o are also listed.

A	$F_1'-F_0$	$F_2''-F_0$	j_0	$\frac{j_a}{j_0}$	$\frac{E_a}{E_0}$
	$-(d_f+d_c)$	(d_f+d_c)			
	2	2	d_f+d_c		
lines/mm	mm	mm	mm		
5	−2.770	2.770	5.540	0.910	0.910
10	−1.510	1.510	3.020	.834	.823
22	−0.825	0.825	1.650	.697	.690
31	− .656	.656	1.312	.619	.607
42	− .547	.547	1.094	.543	.523
64	− .448	.448	0.896	.442	.406
87	− .394	.394	.788	.365	.308
127	− .349	.349	.698	.284	.191
175	− .322	.322	.644	.224	.085
200	− .313	.313	.626	.201	.038
212	− .309	.309	.618	.191	.017
222	− .307	.307	.614	.186	.000

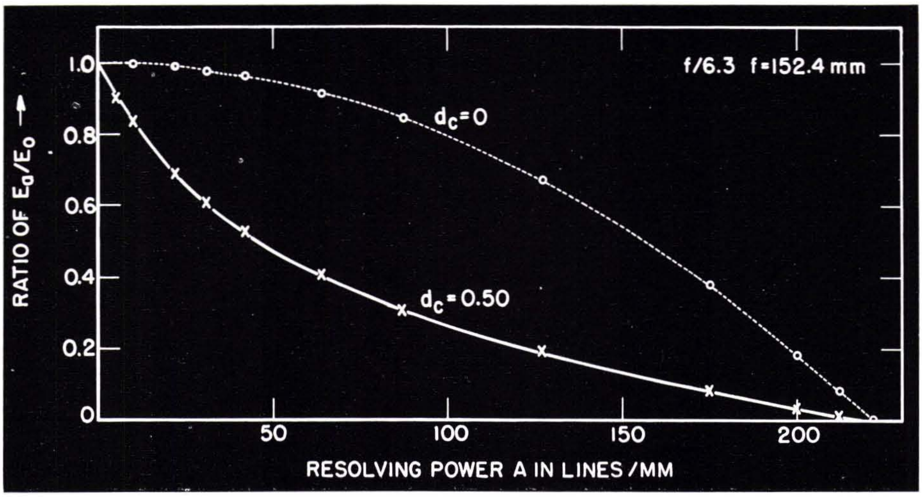

FIG. 7. E_a/E_o *vs*. A for an image plane f_o separated Δf from F_o and lying in the region $-d_c/2 \leq \Delta f \leq d_c/2$ where d_c is the longitudinal chromatic aberration. Results are given for $d_c = 0.00$ and $d_c = 0.50$ mm.

When f_o is displaced by an amount Δf greater than $d_c/2$ from F_o, the region bounded by f_1 and f_2 no longer falls wholly within the bounds F_1' and F_2''. This is illustrated in Figure 6B where $\Delta f = 0.40$ mm. The values of f_1 and f_2 are computed with the aid of Equations 12 and 13 and are listed in Table 4 for the case of $\Delta f = 0.4$ mm.

Following Equation 15,

$$j_a = y_1 x_2' = F_2' - f_1$$

$$= d_f + \frac{d_c}{2} - \Delta f \tag{27}$$

and

$$j_o = x_1' x_2' = d_f + d_c. \tag{28}$$

Using the values of j_a and j_o given by Equations 27 and 28, the values of j_a/j_o may be determined. Values of j_a/j_o for $\Delta f = 0.4$ are listed in Table 4 for each value of A. For values of $\Delta f < (-d_c/2)$, j_a is given by the relation

$$j_a = d_f + \tfrac{1}{2} d_c + \Delta f. \tag{29}$$

TABLE 4

Range of focus as a function of resolving power A for the image plane f_o referred to the plane of best focus F_o (for $\lambda = \lambda_c$) where $\Delta f = f_o - F_o = 0.4$ mm for an $f/6.3$ lens with longitudinal chromatic aberration $d_c = 0.50$ mm. Values of the ratio j_a/j_o and E_a/E_o are also listed.

A	$f_1 - F_o$	$f_2 - F_o$	j_a	j_a/j_o	E_a/E_o
lines/mm	mm	mm	mm		
5	−2.120	2.920	4.890	0.883	0.883
10	−0.860	1.660	2.370	.785	.783
22	− .175	0.975	1.000	.606	.600
31	− .006	.806	0.662	.505	.495
42	.103	.697	.444	.406	.391
64	.202	.598	.246	.275	.252
87	.256	.544	.138	.175	.148
127	.301	.499	.048	.069	.046
175	.328	.472	−.006		
200	.337	.463	−.024		
212	.341	.359	−.032		
222	.343	.357	−.036		

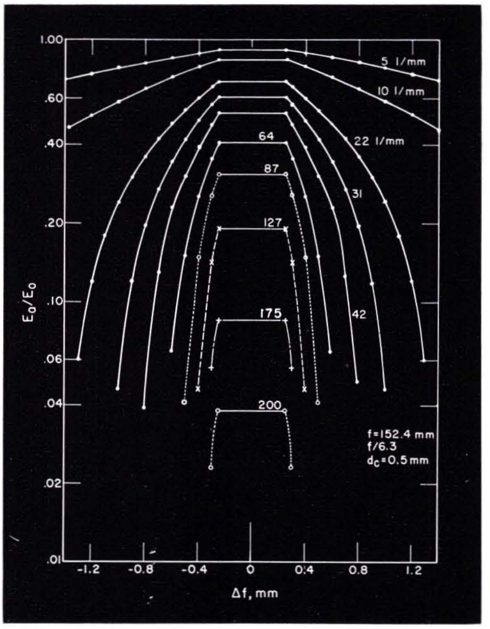

FIG. 8. E_a/E_o *vs*. Δf at selected values of resolving power A. These curves indicate the manner in which contrast in an image of given resolving power varies with displacement of the image plane from the central plane of best focus F_o for a lens having longitudinal chromatic aberration $d_c = 0.50$ mm.

The value of the ratio E_a/E_o can then be computed for all values of d_c and Δf using Equation 21 and values of j_o and j_o from Equations 27, 28 and 29. This has been done for the present case of $b=6.3$ and $d_c=0.50$ and the results are shown in Figure 8 where the values of E_a/E_o are plotted as a function of Δf for a series of values of A. When Figure 8 is compared with Figure 4, it is apparent that longitudinal chromatic aberration can produce marked changes in the value of E_a/E_o. The depth of focus is increased by amount d_c at each value of A and if the ratio E_a/E_o be regarded as closely related to image contrast, the contrast is lowered for all values of A. For the higher values of A, the reduction in contrast may be so great that the apparent limit of resolution A_o is lowered substantially.

4.4 EFFECT OF LONGITUDINAL SPHERICAL ABERRATION

Longitudinal spherical aberration is the variation of the position of best focus with zone height h. It is usually expressed as a displacement $\Delta f'$ from the focal plane for paraxial rays F_o. Measured values of longitudinal spherical aberration for a typical lens of the type described in Table 1 are listed under the heading $(F_o+\Delta f')$ in Table 5. For convenience, the zero of abscissae is shifted so that $F_o=0$. The values of h and A for each value of $\Delta f'$ are also listed in Table 5. It is obvious that this displacement $\Delta f'$ of the position of best focus with zone height h must affect both resolving power and image contrast. The limits of the region of usable imagery, given in Equations 9 and 10, may be modified to include the effects of longitudinal spherical aberration $\Delta f'$ and become

TABLE 5

Region of usable imagery with respect to the plane of best paraxial focus F_o (for $\lambda=\lambda_c$) as a function of resolving power A vs $\Delta f=(f_o-F_o)$ for an $f/6.3$ lens having longitudinal spherical aberration $\Delta f'$. The values of the zone height h corresponding to the listed values of A are also given.

A	Zone height h	$F_o+\Delta f'$	$F_1'-F_o$	$F_2''-F_o$	$\frac{F_2''-F_1'}{j_o}$
lines/mm	mm	mm	mm	mm	mm
5	0.3	0.00	−2.520	2.520	5.040
10	.6	.00	−1.260	1.260	2.520
22	1.2	−.03	−0.605	0.545	1.150
31	1.7	−.11	− .516	.296	0.812
42	2.3	−.18	− .477	.117	.594
64	3.5	−.27	− .468	−.072	.396
87	4.8	−.49	− .634	−.346	.288
127	6.9	−.68	− .779	−.581	.198
175	9.5	−.69	− .762	−.618	.144
200	10.9	−.46	− .523	−.397	.126
212	11.5	−.40	− .459	−.341	.118
222	12.1	− 34	− .397	−.283	.114

TABLE 6

Region of usable imagery with respect to the plane of best paraxial focus F_o (for $\lambda=\lambda_c$) as a function of A vs Δf for an $f/6.3$ lens having longitudinal chromatic aberration $d_c=0.50$ mm and longitudinal spherical aberration $\Delta f'$ as listed in Table 5. The values of j_o are also listed.

A	$F_1'-F_o$	$F_2''-F_o$	$\frac{F_2''-F_1'}{j_o}$
lines/mm.	mm	mm	mm
5	−2.770	2.770	5.540
10	−1.510	1.510	3.020
22	−0.855	0.795	1.650
31	− .766	.546	1.312
42	− .727	.367	1.094
64	− .718	.178	0.896
87	− .884	−.096	.788
127	−1.029	−.331	.698
175	−1.012	−.368	.644
200	−0.773	−.147	.626
212	− .709	−.091	.618
222	− .647	−.033	.614

$$F_1' = F_o - d_f/2 - \Delta f' = F_o - 2b/A - \Delta f' \quad (30)$$

and

$$F_2'' = F_o + d_f/2 - \Delta f' = F_o + 2b/A - \Delta f'. \quad (31)$$

The shape of the region of usable imagery bounded by F_1 and F_2 as illustrated in Figure 2A is altered or warped by the inclusion of the $\Delta f'$ values which also vary with h or A. Values of F_1' and F_2'' for an $f/6.3$ lens having the values of longitudinal spherical aberration $\Delta f'$ listed under the heading $(F_o+\Delta f')$ in Table 5 have been calculated with the aid of Equations 30 and 31 and are also listed in the table.

When longitudinal chromatic aberration d_c and longitudinal spherical aberration $\Delta f'$ are both present the limits of the region of usable imagery are altered still further but may be defined by modified forms of Equations 22 and 23 as follows

$$F_1' = F_o - \tfrac{1}{2}(d_f + d_c) - \Delta f' \quad (32)$$

and

$$F_2'' = F_o + \tfrac{1}{2}(d_f + d_c) - \Delta f'. \quad (33)$$

The values of j_a used in the ratio j_a/j_o may be determined in the manner shown in Sections 4.2 and 4.3 except that these values are affected by the presence of the longitudinal spherical aberration $\Delta f'$.

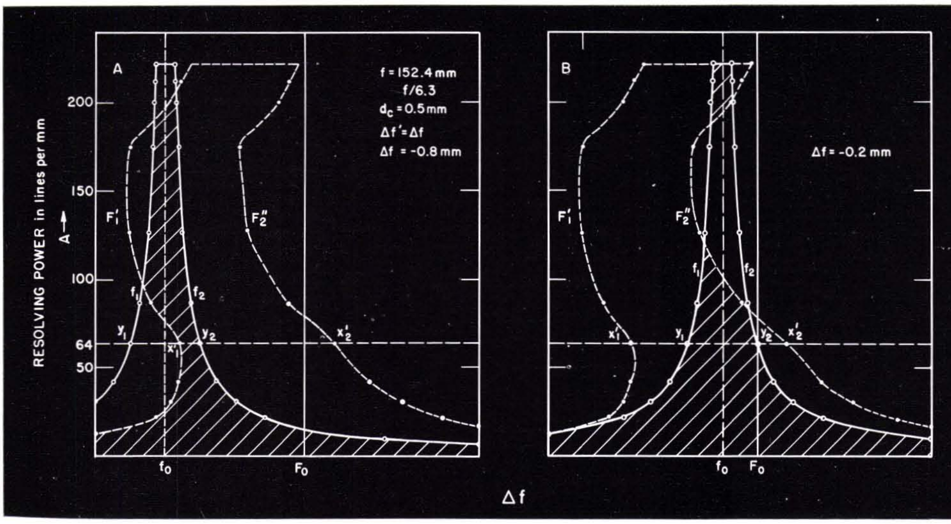

FIG. 9. Axial resolving power A *vs.* Δf for a lens affected by both longitudinal chromatic aberration d_c and longitudinal spherical aberration $\Delta f'$. Curves F_1' and F_2'' mark the bounds of the region of usable imagery. F_o marks the location of the plane of paraxial focus for $\lambda = \lambda_c$. For an image plane f_o distant Δf from F_o, the curves f_1 and f_2 show the limiting depth of focus with respect to f_o for each value of A. In Box A, the shaded area shows the region of usable imagery common to f_o and the region enclosed by F_1' and F_2'' for $\Delta f = (f_o - F_o) = -0.8$ mm. Similar information for $\Delta f = -0.2$ mm. is shown in Box B.

To illustrate the method of analysis leading to the determination of E_a/E_o for any image plane of a lens affected by both longitudinal and chromatic aberration, values of F_1' and F_2'' have been calculated for an $f/6.3$ lens having $d_c = 0.50$ mm and $\Delta f'$ as listed in Table 5. These values of F_1' and F_2'' are listed in Table 6 together with the value of j_o from Equation 28. These values are also shown in Figure 9. Comparison of Figures 5 and 9 demonstrates clearly the distortion of the region of usable imagery resulting from longitudinal spherical aberration. To determine the manner in which E_a/E_o varies with A in a plane f_o distant $\Delta f = f_o - F_o$ from the plane of best paraxial focus, values of f_1 and f_2 are determined with the aid of Equations 12 and 13 and are used as indicated in Equations 17 and 18 to obtain the focal depth common to the region bounded by f_1 and f_2 and that bounded by F_1' and F_2'. Values of f_1 and f_2 for $\Delta f = -0.8$ are listed in Table 7 and are shown graphically in Figure 9. Values of j_a and j_a/j_o are also listed in the table. For this case, the values of E_a/E_o using these values of j_a/j_o in Equation 21 have been computed and are listed in Table 7. Values of E_a/E_o for $\Delta f = -0.8$ are also shown in Figure 11.

Values of j_a/j_o and E_a/E_o have been computed in the present case for a series of focal planes at 0.1 mm intervals over the range from $\Delta f = -1.2$ to $\Delta f = 1.2$.

The values of E_a/E_o vs Δf for Δf ranging from -1.2 to 1.2 mm are shown for a series of values of A in the Frontispiece. When the Frontispiece is compared with Figure 8, it is apparent that the addition of longitudinal spherical aberration produces marked changes in the manner that E_a/E_o varies with Δf. The values of E_a/E_o as a function of A for 12 different positions of the image plane are shown in Figure 10. From curves such as shown in the Frontispiece and Figure 10 it is clear that there may be a shift in the plane of best focus

TABLE 7

Range of focus as a function of resolving power A for the image plane f_o with respect to the plane of best paraxial focus F_o (for $\lambda = \lambda_c$) where $\Delta f = (f_o - F_o) = -0.8$ mm for a lens having longitudinal chromatic aberration $d_c = 0.50$ mm and longitudinal spherical aberration $\Delta f'$ as listed in Table 5. Values of j_a, j_a/j_o, and E_a/E_o are also listed.

A	$f_1 - F_o$	$f_2 - F_o$	j_a	j_a/j_o	E_a/E_o
lines/mm	mm	mm	mm		
5	−3.320	1.720	4.490	0.810	0.810
10	−2.060	0.460	1.970	.652	.651
22	−1.375	−.225	0.630	.382	.378
31	−1.206	−.394	.372	.284	.278
42	−1.097	−.503	.224	.205	.197
64	−0.998	−.602	.116	.129	.119
87	− .944	−.656	.228	.289	.244
127	− .899	−.701	.198	.284	.191
175	− .872	−.728	.144	.224	.085
200	− .863	−.737	.036	.058	.011
212	− .859	−.741	.000	.000	.000
222	− .857	−.743	.000	.000	.000

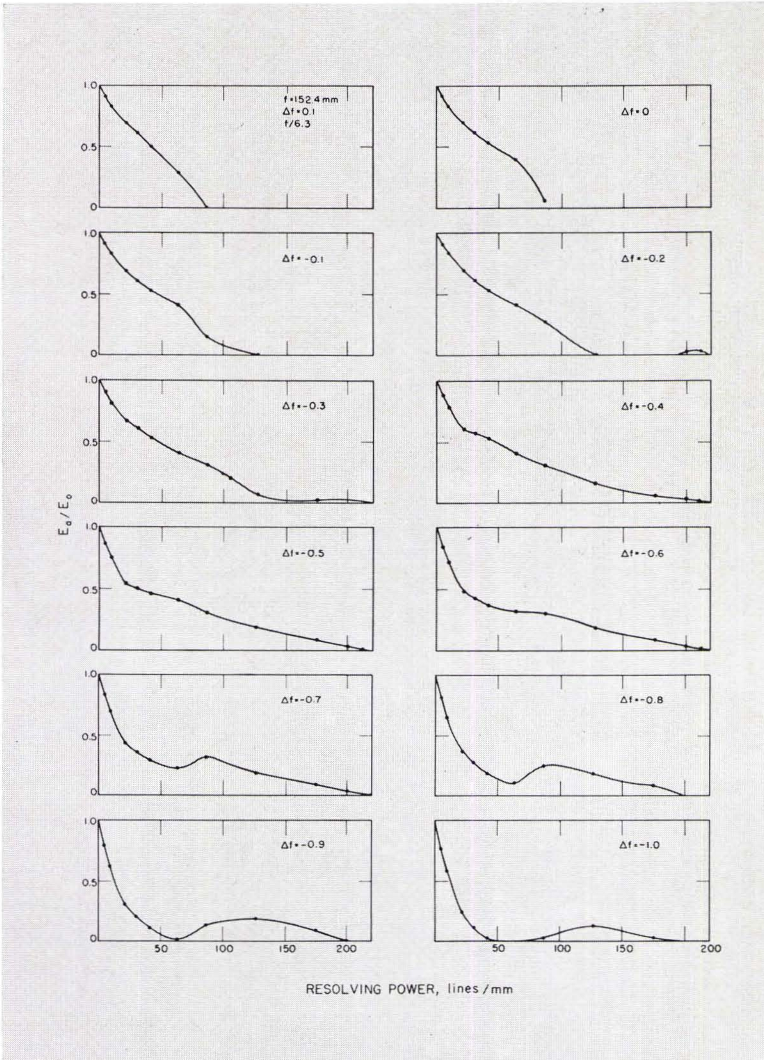

FIG. 10. E_a/E_o *vs.* A for 12 positions of the image plane. These curves show the manner in which image contrast varies with resolving power in a series of image planes spaced at 0.1 mm intervals through the range of Δf from $\Delta f=0.1$ to $\Delta f=-1.0$ mm for a lens having longitudinal chromatic aberration $d_c=0.50$ mm and longitudinal spherical aberration $\Delta f'$ as given in Table 5.

with changing values of the resolving power A. It is clear also that when one selects the plane yielding maximum contrast at low values of A, it may not be possible to obtain high values of A in the same plane, while a plane characterized by maximum contrast at a moderately high value of A will still yield resolution with relatively small loss of contrast at the low values of A.

It is worthy of note that the curves shown in the Frontispiece show a striking resemblance to curves reported for similar lenses[5] which show measured contrast vs displacement Δf from the position of best axial focus for a series of values of the resolving power A. In addition the curves shown in Figure 10 show a marked resemblance to curves reported for a similar lens[6] which show variation contrast for a series of focal positions.

4.5 COMPARISON OF MEASURED AND THEORETICAL VALUES OF RESOLVING POWER THROUGHOUT THE REGION OF USABLE IMAGERY

In Figure 11, Curve 1 shows the region of usable imagery determined by the measured values of resolving power as a function of Δf, the measured displacement from the plane

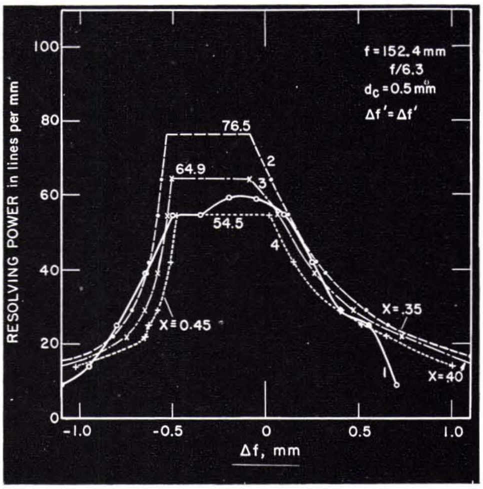

FIG. 11. Comparison of theoretical and measured values of resolving power *vs.* Δf for the region of usable imagery for a lens having chromatic aberraion $d_c=0.5$ mm and spherical aberration $\Delta f'=\Delta f'$. Curve 1 shows A *vs.* Δf measured from the plane of best axial focus for an actual lens obtained photographically with a fine grained emulsion. Curves 2, 3 and 4 are theoretical curves of A *vs.* Δf for three different values of E_a/E_o. For Curve 2, $E_a/E_o=0.35$; for Curve 3 $E_a/E_o=0.40$; and for Curve 4, $E_a/E_o=0.45$. The maximum theoretical values of A for these values of E_a/E_o are indicated on the curves.

of best visual focus. These values of A were determined photographically in the manner described in Section 3. The values of longitudinal chromatic aberration d_c and longitudinal spherical aberration $\Delta f'$ for this same lens were measured and are the values used in the illustrative examples given in Section 4.3 and 4.5. It is therefore of interest to determine the form of the curve of A *vs* Δf that may be inferred at a series of fixed values of E_a/E_o determined as shown in Section 4.4. To do this one determines for a series of values of A values of Δf for which the value of E_a/E_o has a specific preselected value. When this is done the values of A plotted against Δf form a curve bounding a region of usable imagery for which the minimum value of E_a/E_o is the preselected value.

Curves are obtained in the foregoing manner for three values of E_o/E_o are shown as Curves 2, 3, and 4 in Figure 11. The values of E_a/E_o for these three cases are (2) 0.35, (3) 0.40, and (4) 0.45. The maximum possible resolving powers for these three conditions are indicated on the curves as 76.5, 64.9, and 54.5 lines/mm. It is clear that the curve marked (4) for which $E_a/E_o=0.40$ closely approximates the curve marked 1 which shows the measured value of A *vs* Δf. One might infer from this close resemblance of the theoretical curve of A *vs* Δf for $E_a/E_o=0.4$ and the curve of measured values of A *vs* Δf, that when one has available the measured values of d_c and $\Delta f'$ for a given lens a reasonably good prediction can be made concerning the probable values of the resolving power that might be obtained with that lens throughout the region of usable imagery under conditions similar to those present for Curve 1.

5.0 SUMMARY

This paper presents a method whereby the probable values of resolving power of a lens throughout the region of usable imagery can be predicted provided reliable values of the longitudinal chromatic and longitudinal spherical aberration are known for the particular lens. A numerical index has been developed expressed as the ratio E_a/E_o which is derived from aperture area, depth of focus, longitudinal chromatic and longitudinal spherical aberration which varies from 1 to 0 as the resolving power A varies from 0 to its maximum A_o. This index appears to be directly proportional to contrast in the image and the manner of its development indicates that the observable variations in contrast *vs* resolving power can be accounted for by these aberrations plus displacement of the image plane in a similar manner.

6.0 ACKNOWLEDGEMENTS

The author expresses appreciation to other members of the staff of the National Bureau of Standards for assistance during this work and in particular to Mr. E. C. Watts who prepared the illustrations.

7.0 REFERENCES

1. Region of usable imagery in airplane-camera lenses. F. E. Washer. *J. Research NBS 34,* 175 (1945) RP1636.
2. Method for determining the resolving power of photographic lenses. F. E. Washer and I. C. Gardner. *NBS Circular* 533 (1953).
3. Variation of resolving power and type of test pattern. F. E. Washer and W. P. Tayman. *J. Research NBS 64C,* 209 (1960).
4. Measurement of longitudinal spherical aberration in the extra-axial region of lenses. F. E. Washer and W. R. Darling. *J. Research NBS 66C,* 185 (1962).
5. Effect of object frequency on focal position of four photographic objectives. F. W. Rosberry. *J. Research NBS 57,* 17 (1956).
6. Equipment and method for photoelectric determination of image contrast suitable for using square wave targets. F. W. Rosberry, *J. Research NBS 64C,* 57 (1960).